Rare Metal Materials and Engineering
Volume 43, Issue 2, February 2014
Online English edition of the Chinese language journal

Available online at www.sciencedirect.com
ScienceDirect

Cite this article as: Rare Metal Materials and Engineering, 2014, 43(2): 0264-0268.

ARTICLE

Effect of Mo Content on the Structural and Mechanical Properties of CrMoN/MoS$_2$ Composite Coatings

Di Yuelan, Zhang Ping, Cai Zhihai, Yang Zhen, Li Qi, Shen Wei

Academy of Armored Forces Engineering, Beijing 100072, China

Abstract: CrMoN/MoS$_2$ composite coatings were prepared on the surfaces of the CrMoN composite coatings with different Mo contents by means of a low temperature ion sulfurizing process. The structural and mechanical properties of these coatings as a function of Mo content have been studied. SEM analysis shows that the CrMoN coating reveals a dense and compact surface structure, the CrMoN/MoS$_2$ composite coatings display loose grain structures; In the sulfurizing process, a preferential growth does not happen, the sulfide size is inhibited, The products of the reaction between MoN$_x$ and S are the main origin of MoS$_2$.Nanoindentation test shows that the hardness and Young's modulus of CrMoN/MoS$_2$ coatings are higher than that of CrMoN composite coatings.

Key words: CrMoN/MoS$_2$ composite coating; microstructure; mechanical property

CrN is an important coating material for its corrosion resistance, oxidation protection properties and a good wear resistance, and has been used as a protective coating on tools in applications such as cutters, grinding tools and piston rings[1,2]. However, the main drawback for the use of CrN is still its hardness (18 GPa)[3],which even if it is relatively high, is not good enough to compete with that of TiN (21~23 GPa)[4]. Ternary Cr-Mo-N coatings can have superior properties tailored through appropriate combinations of CrN and MoN. The Cr-Mo-N coatings showed an increased hardness value of approximately 34 GPa at 21 at% Mo, compared with 18 GPa for pure CrN, and the friction coefficient decreased from 0.49 for pure CrN coating to 0.37 for Cr-Mo-N with 30.4 at% Mo[5]. However, the friction coefficients of the Cr-Mo-N composite films were limited in some extent for the formation of MoO$_3$ phase as a lubricant during the friction process[6,7]. And it can't meet the needs of the rigorous working circumstance of parts (such as piston rings) for its limited lubricant effects.

MoS$_2$ has a 2-D layered crystalline structure[8] which provides low shear strength along its basal planes, its coefficient of friction is low and can be as low as 0.01[9] in vacuum. Therefore, MoS$_2$ is mostly used in vacuum and environments free of water vapor. It is interested in depositing an interlayer between the substrate and the MoS$_2$ coating for improving the tribological properties of MoS$_2$ coatings[10].

In this paper, CrMoN/MoS$_2$ composite coatings were prepared by combining magnetron sputtering and low temperature ion sulfurizing technology. And the correlation about the Mo contents and the structures and the mechanical properties of CrMoN/MoS$_2$ composite coatings were studied.

1 Experiment

CrMoN/MoS$_2$ coatings were prepared in two steps. First, the Cr-Mo-N coatings with different Mo contents were deposited using TEER UDP-650 closed-field unbalanced magnetron sputtering coater. The 65Mn steel wafers with 40 mm (length)×30 mm (width)×1 mm (height) and a silicon (100) wafer were used as substrates, they were hung on the work rest. A rotating substrate holder which could provide a uniform exposure for growing the film was surrounded by four vertically mounted pure metallic targets (Cr, Mo). The rotational speed of the substrate was 4 r/min. The target-to-substrate distance was 12 cm. Ar gas (99.999%) was introduced into the sputter target holder to increase the sputtering rate and N$_2$ gas (99.999%) which controlled by Optical Emission Monitor was injected near the substrate holder. Be-

---

Received date: March 25, 2013
Foundation item: National Natural Science Foundation of China (50901089); National Key Laboratory for Remanufacturing under Grant (9140C850207100C8506)
Corresponding author: Di Yuelan, Candidate for Ph. D., Depart of Equipment Remanufacturing Engineering, Academy of Armored Forces Engineering, Beijing 100072, P. R. China, Tel: 0086-10-66719249, E-mail: dylxinjic031@c163.com

Copyright © 2014, Northwest Institute for Nonferrous Metal Research. Published by Elsevier BV. All rights reserved.

fore deposition, the inside of deposition chamber was evacuated less than 2.0×10^{-3} Pa for all deposition, the deposition parameters were as follows: sputtering chamber pressure, 0.133 Pa, substrate temperature, less than 500 ℃. Cr target current was fixed, and Cr-Mo-N ternary films of different Mo content were prepared by adjusting Mo target current.

Secondly, the Cr-Mo-N coatings were then treated by low temperature ion sulfuration in the equipment of model DW-1 for 2 h. The reacting gas was coming from the solid sulfur. When the vacuum was up to a certain value, the ammonia gas was filled into the chamber. The direct current was applied between the cathode and anode to ionize the ammonia gas, the ammonia ions were accelerated to bombard the cathode (workpieces), elevating their temperature. Till the temperature was up to a scheduled value of 230 ℃, bombardment stopped.

The morphologies of the coatings were observed by a field-emission scanning electron microscope (FESEM).The chemical composition of the micro particles in the film were measured by X-ray energy dispersion spectroscopy system. The phases and crystallization of the samples were identified by X-ray diffraction analysis with a diffract meter using Cu radiation. The X-ray photoelectron spectroscopy (XPS) measurement was carried out by an ESCALAB 250iXL (V G Scientific) type spectrometer. Scanning Augur Microprobe (AES) was utilized to analyze the distribution of elements along with depth. The hardness of multilayer films was measured by using multi-function nanotest 600 hardness- testing devices.

2 Results and Discussion

2.1 Composition and Phase structure

The compositions of the CrMoN/MoS_2 coatings are shown in Table.1. It can be seen that as the Mo target current increases from 1 to 5 A, the Mo content in the CrMoN coating increases from 11.42 at% to 33.27 at%, with a corresponding decrease of Cr from 38.63 at% to 17.07 at%. The nitrogen content is almost constant in the coating for 50 at%. The atomic percentage of N element is equal to the atomic percentage sum of Cr element and Mo element, according to chemical measurement ratio, the chemical formula can be expressed for $Cr_{1-x}Mo_xN$, x=Mo/(Cr+Mo). The composite of Cr and Mo elements decrease a little after sulfurizing. The S contents in CrMoN/MoS_2 coatings increases with the increasing of Mo current. During sulfurizing processing, CrMoN coatings fixed at cathode are bombarded by ammonia ions, partial Cr ions and Mo ions are sputtered out of CrMoN coatings, S atom is then permeated along defects and grain boundary.

The XRD pattern of the CrMoN coating and CrMoN/MoS_2 coating are shown in Fig.1. From Fig.1, the broadened peaks are observed in (111), (200), (220) and (311) crystal planes of both CrN and γ-Mo_2N phases for the Cr-Mo-N coating. A strong peak centered at approximately 2θ=33.8°, which corresponds to the (100) plane of molybdenum sulfide and chromium sulfide (Fig.2). The peak centered at 2θ=57° was broadened, which may be resulted in amorphous MoS_2. Also, the peak centered at 2θ=76° was broadened, which may be attributed to the distortion of lattice resulted in grain refining or solid solution phase in the coatings. Compared with Cr-Mo-N coating, the MoS_2 and Cr_2S_3 phase were occurred after sulfurizing.

Table 1 Compositions of CrMoN/MoS_2 coatings (at%)

I_{Mo}/ A	CrMoN		CrMoN/MoS_2			x=Mo/
	Cr	Mo	Cr	Mo	S	(Cr+Mo)
1	38.63	11.42	37.58	10.97	1.5	0.23
2	31.75	18.87	30.9	17.54	2.18	0.37
3	25	26.48	22.51	24.11	3.38	0.51
4	20.72	30.69	19.16	27.29	4.96	0.6
5	17.07	33.27	14.93	28.17	6.9	0.65

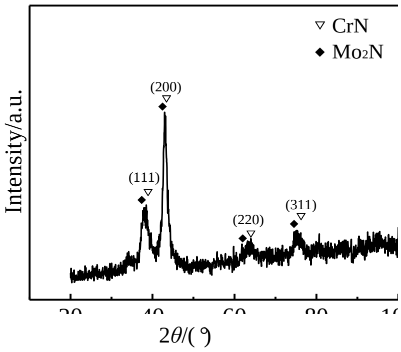

Fig.1 XRD pattern of CrMoN coating

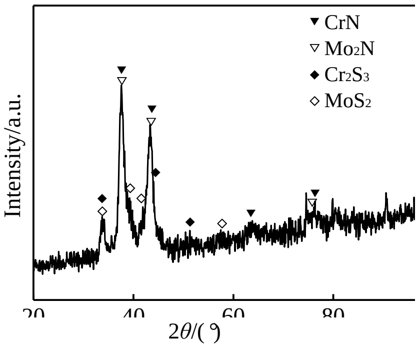

Fig.2 XRD pattern of CrMoN/MoS_2 coating

2.2 XPS analysis

The XPS analysis results of the chemical valence states of CrMoN/MoS_2 coatings are shown in Fig.3. The peaks of Cr 2p are the compounds of Cr-S, Cr-N and Cr-O, where the bonding energies are 574.4, 575.3 and 576.8 eV, respectively. The appearance of Cr-O may be attributed in surface oxide pollution. The peak of Mo emerges in the place where Mo (228 eV) and Mo-S (229 eV) are superposed. The peak of Mo-N is corresponding to the bonding energy of 231.5 eV. In S2p, Cr-S and Mo-S correspond to 161.3 and 162.5 eV, respectively.

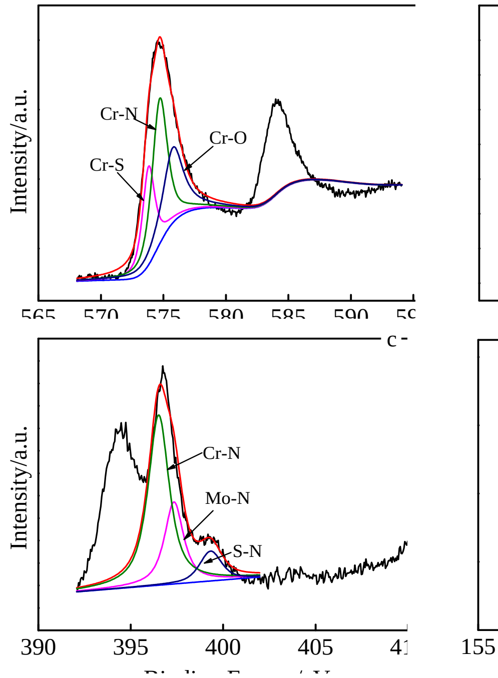

Fig.3 XPS analysis of CrMoN/MoS_2 coatings: (a) Cr 2p, (b) Mo 3d, (c) N 1s, and (d) S 2p

Besides, S-N also can be observed but is less, so it cannot be displayed in XRD results.

Table 2 shows the function of Mo content and the XPS analyses of Mo element. The content of MoO_3 can be ignored for its small quantities. It can be seen that the contents of MoN_x are more than Mo contents. After sulfurizing, both of them decrease, while MoS_2 increases. The sulfuration reaction is analyzed by thermodynamic theory to explore the formation origin of MoS_2.

Two reactions of Mo and S maybe happen in sulfurizing processing:

$$Mo+S_2 \rightarrow MoS_2 \quad (1)$$

$$2Mo_2N+3S_2 \rightarrow 2MoS_2+2SN \quad (2)$$

The enthalpy and the entropy of reactants and products in reactions (1) and (b) are calculated as follows:

Reaction (1):

$$\Delta G_{\mathrm{T}}^{\theta} = \Delta H_{298.15-\mathrm{T}}^{\theta}\Delta S_{298.15}^{\theta} = -276.144-1.944T<0 \quad (3)$$

Reaction (2):

$$\Delta G_{\mathrm{T}}^{\theta} = \Delta H_{298.15-\mathrm{T}}^{\theta}\Delta S_{298.15}^{\theta} = -941.4-346.846T<0 \quad (4)$$

Table 2 Function of Mo content and XPS analyses of Mo element (at%)

Coating	CrMoN		CrMoN/MoS_2		
	Mo	MoN_x	Mo	MoN_x	MoS_2
$Cr_{0.77}Mo_{0.23}N$	40.05	59.95	24	44.5	31.5
$Cr_{0.63}Mo_{0.37}N$	41.89	58.11	27.27	37.45	35.28
$Cr_{0.49}Mo_{0.51}N$	43.73	56.27	28.13	29.65	42.22
$Cr_{0.4}Mo_{0.6}N$	44.07	55.95	29.12	22.48	48.4
$Cr_{0.35}Mo_{0.65}N$	43.91	56.1	32.6	15.25	52.15

Therefore, the two reactions are feasible in set temperature, and the products of reaction between MoN_x and S are the main origin.

2.3 Morphology

The surface morphologies of CrMoN and CrMoN/MoS_2 coatings are shown in Fig.4. It can be seen that the morphology of CrMoN coating is entirely different to those of CrMoN/MoS_2 composite coatings. The CrMoN coating displays a dense and compact surface structure; the grains are large while CrMoN/MoS_2 coatings exhibit porous and loose structures, which is caused by a nonreactive nucleation. In the sulfurizing process, the sulfides growth peripherally after nucleation, then meet other sulfides which growth with other nucleation particles, a preferential growth does not happen in the growth process, the sulfide size is inhibited, and finer and granular grains can be seen in the figure.

2.4 AES analysis

The distribution of elements of CrMoN sulfurized coatings with different Mo contents are shown in Fig.5. Owing to sulfide layer oxidizing being easy, carbonyl pollution layers with 3~8 nm are formed on the surfaces of coatings. In $Cr_{0.77}Mo_{0.23}N$ coatings, the atom mol ratio of S and Mo is larger than 1 at the displacement into the surface of 14 nm, which indicates the existence of sulfur-enriched layer on the coating surface. While the atom mol ratio is smaller than 1 at the displacement into surface of 40 nm, S content decreases to zero. According to the analysis, the sulfuration layers consist of a sulfur-enriched layer and a diffusion layer, and the depth of the sulfuration layer increases with the increase of Mo content. In $Cr_{0.35}Mo_{0.65}N$ coating, the sulfuration layer is 120 nm.

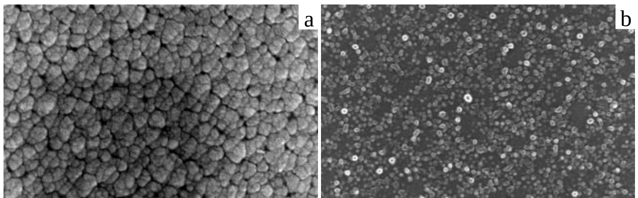

Fig.4 Surface morphologies of CrMoN (a) and CrMoN/MoS_2 (b) coatings

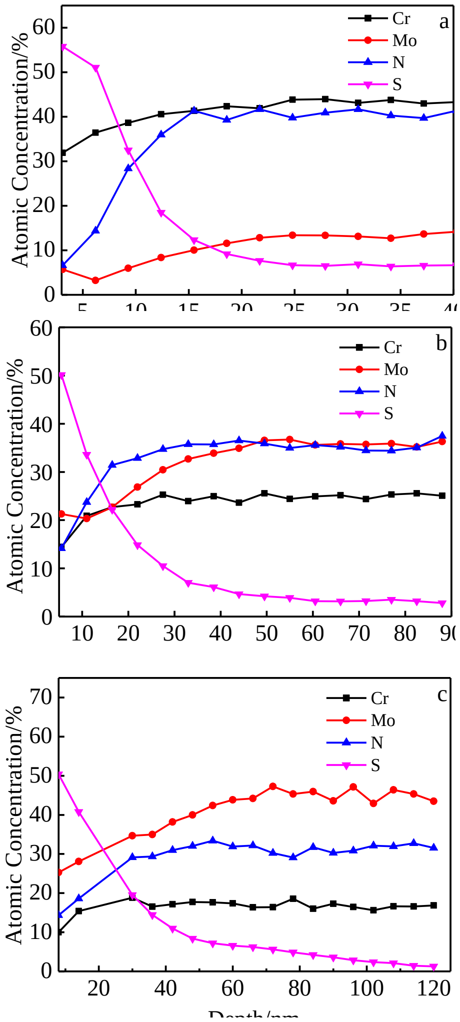

Fig.5 AES analysis of coatings: (a) $Cr_{0.77}Mo_{0.23}N$, (b) $Cr_{0.49}Mo_{0.51}N$, and (c) $Cr_{0.35}Mo_{0.65}N$

2.5 Nanoindentation

The nanohardness and Young's modulus of the CrMoN/MoS_2 composite coating are shown in Fig.6. The results are the average values in the range of 300~400 nm distance into a surface. It can be seen that the nanohardness and Young's modulus of CrMoN/MoS_2 composite coating are higher than those of CrMoN coating, and increase with the increasing of Mo content. The reason can be analyzed as follows: (1) fine grained strengthening. The refinement of grains of CrMoN/MoS_2 composite coating creates more dislocations at the grain boundaries, the sizes of grains of surface layer are less than 30 nm; (2) symplesitc growth. During sulfurizing process, S atom come in the intracell and replace N atom to form MoS_2, which strengthen the interformational bonding force. A crystallization MoS_2 usually has lower hardness, an amorphous MoS_2 has relatively high hardness, such as MoST coating prepared by TEER Co. with more 20 GPa. So, the relatively higher hardness of the CrMoN/MoS_2 composite coatings may be the formation of the amorphous MoS_2 in the coatings. The existence of CrN and MoN phases can stand MoS_2 soft phase, the interphase interaction of the hard phase and the soft phase can improve mechanical properties of CrMoN/MoS_2 composite coatings.

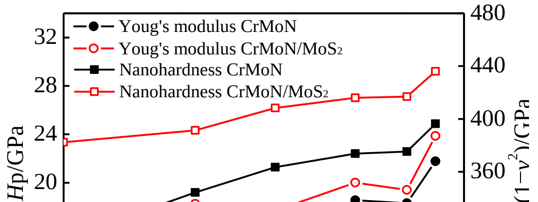

Fig.6 Nanoindentation results of CrMoN/MoS_2 composite coatings with different Mo content

3 Conclusions

1) The CrMoN coating exhibits a dense and compact surface structure with larger; grains, while CrMoN/MoS_2 coatings display porous and loose structures, which is caused by nonreactive nucleation. In the sulfurizing process, the preferential growth does not happen, the sulfide size is inhibited, and grains are refined, resulting in increasing of the hardness.

2) A composite phase structure can be formed on the surface of CrMoN/MoS_2 composite coating after sulfurizing. The outer surface is MoS_2 with an antifriction and lubricant effects, and the subsurface is CrN and Mo_2N with high hardness. The products of the reaction between MoNx and S are the main origin of MoS_2.

3) The nanohardness and Young's modulus of CrMoN/MoS_2 composite coating are higher than those of CrMoN coating, and increases with increasing of Mo content.

References

1 Pradhan S K, Nouveau C, Vasin A *et al. Surface and Coatings Technology*[J], 2005, 200(1-4): 141

2 Polcar T, Parreira N M G, Novák R. *Surface and Coatings Technology*[J], 2007, 201: 5228

3 Bull S J, Rickerby D S. *Surf Coat Technol*[J], 1990, 732: 43

4 Yashar P, Barnett S A, Rechner J *et al*. *Sci Technol A*[J], 1998, 16: 2913

5 Hones P, Sanjines R, Levy F *et al*. *Sci Technol A*[J], 1999, 17(3): 1024

6 Eun Young Choia, Myung Chang Kangb. *Journal of Materials Processing Technology*[J], 2007, 187-188(3): 566

7 Kwang Ho Kima, Eun Young Choia, Seung Gyun Honga. *Surface and Coatings Technology*[J], 2006, 201(2): 4068

8 Cong D Y, Wang J, Ou Y J. *Thin Solids Films*[J], 1992, 2: 209

9 Weise G, Teresiak A, Bacher I *et al*. *Surf Coat Technol A*[J], 1994, 12: 1998

10 Xu G Z, Zhou Z R, Liu J J *et al*. *Wear*[J], 1999, 225-229: 46

Mo 含量对 CrMoN/MoS$_2$ 复合涂层的组织结构及力学性能的影响

底月兰，张平，蔡志海，杨臻，李奇，沈维

(装甲兵工程学院，北京 100072)

摘要： 通过对不同Mo含量的CrMoN复合涂层进行低温离子渗硫处理获得CrMoN/MoS$_2$复合涂层，并对其组织结构及力学性能进行研究。扫描电镜分析显示出CrMoN复合涂层表面形貌比较致密，晶粒较大，而经过渗硫处理后的CrMoN/MoS$_2$复合涂层呈现了疏松的颗粒状的形貌。由于渗硫过程是非反应成核扩散过程，期间没有发生择优生长，故晶粒尺寸受到抑制。对渗硫过程中可能发生的反应进行热力学计算，推断复合涂层中的Mo单质和MoN$_x$均可与S元素发生反应生成MoS$_2$，通过对CrMoN/MoS$_2$复合涂层表面元素的化合价态进行分析，可知MoS$_2$主要来源于MoN$_x$与S发生的置换反应。纳米硬度测试结果表明，渗硫处理后的CrMoN复合涂层的纳米硬度和弹性模量都得到提高，力学性能得到提升。

关键词： CrMoN/MoS$_2$ 复合涂层；组织结构；力学性能

作者简介：底月兰，女，1986 年生，博士生，装甲兵工程学院装备再制造重点实验室，北京 100072，电话：010-66719249，E-mail: dylxinjic031@163.com